Organometallics **1992**, *11*, 589–597

Electrochemical, Spectroscopic, and Structural Studies of Mono- and Bimetallic Complexes of Iron: X-ray Crystal Structures of $CpFe(CO)_2\text{-}C_6F_5$, 4-$CpFe(CO)_2\text{-}C_5F_4N$, and 1,4-$C_6F_4(CpFe(CO)_2)_2$[1–4]

Roxton Chukwu, Allen D. Hunter,* and Bernard D. Santarsiero

Department of Chemistry, University of Alberta, Edmonton, Alberta, Canada T6G 2G2

Simon G. Bott

Department of Chemistry, University of North Texas, Denton, Texas 76203

Jerry L. Atwood and Jeanne Chassaignac

Department of Chemistry, University of Alabama, Tuscaloosa, Alabama 35487

Received July 8, 1991

The oxidative electrochemical behavior of 18 mono- and bimetallic complexes in which $(\eta^5\text{-}C_5H_5)Fe(CO)_2$ (Fp) groups are σ-bound to arene and azine rings has been determined by cyclic voltammetry (CH_2Cl_2, $n\text{-}Bu_4NPF_6$, Pt electrodes) and is described. The oxidation potentials and reversibilities of these compounds are found to be very dependent on the structures of the aromatic ligands. In particular, it was found that the addition of fluorine substituents increased both the oxidation potentials and chemical reversibilities for the aryl complexes, as did the substitution of a nitrogen atom for a C–X group in the aromatic ring. For the bimetallic arene-bridged complexes, the perhydro derivatives (i.e. 1,3- and 1,4-$C_6H_4Fp_2$) show low chemical reversibilities, while the fluorinated bimetallics (i.e. 1,3- and 1,4-$C_6F_4Fp_2$) are reversibly oxidized in two sequential one-electron steps with separation between their first and second oxidations (i.e. $\Delta E_{1/2} = |E^{\circ\prime}_{+1/+2} - E^{\circ\prime}_{0/+1}|$) of 280 and 200 mV for the para- and meta-substituted complexes, respectively. This is indicative of substantial long-range metal–metal electronic coupling in these compounds. The first oxidations for these complexes are much more chemically and electrochemically reversible than are the second oxidations, which are accompanied by complex electrode/electrolyte interactions. For the azine complexes, we find that those species having the Fp substituents ortho to a nitrogen atom are irreversibly oxidized at scan rates of up to 10 V s^{-1}, while the para-substituted halopyridine complexes show excellent chemical reversibilities. The X-ray crystal structures of the title complexes $CpFe(CO)_2\text{-}C_6F_5$, ($C_{13}H_5F_5FeO_2$; a = 6.993 (2) Å, b = 12.774 (4) Å, c = 13.649 (3) Å, V = 1219 Å^3; orthorhombic; *Pnma*; Z = 4), 4-$CpFe(CO)_2\text{-}C_5F_4N$, ($C_{12}H_5F_4FeNO_2$; a = 6.948 (1) Å, b = 12.828 (1) Å, c = 13.000 (1) Å, V = 1159 Å^3; orthorhombic; *Pnma*; Z = 4), and 1,4-$C_6F_4(CpFe(CO)_2)_2$ ($C_{20}H_{10}F_4Fe_2O_4$; a = 7.714 (1) Å, b = 9.840 (1) Å, c = 12.473 (1) Å, β = 107.822 (7)°, V = 901 Å^3, monoclinic; $P2_1/c$; Z = 2) have been determined. In each case, the $CpFe(CO)_2$ group is oriented such that its mirror plane (complexes **6** and **10**) or pseudo mirror plane (complex **3**) is perpendicular to the arene or azine ring rather than parallel to it as predicted by molecular orbital arguments. It is suggested that these unexpected orientations minimize unfavorable steric interactions between the *o*-fluorine substituents on the aromatic groups and the H atoms on the C_5H_5 group of Fp.

Introduction

Because of their potential in practical applications,[7] there has recently been increasing interest in the study of polymeric materials which incorporate transition-metal atoms in the polymer backbone. Since problems such as solubility often hamper systematic studies of such materials, attention has also been directed toward optimizing the magnitudes of the metal–metal interactions in low-molecular-weight model compounds having structures similar to the repeat units of the target polymers.[8,9] As our contribution to this area, we have been studying a series of azine- and arene-bridged organometallic complexes, e.g.

---

(1) Organometallic Complexes with Electronic Bridges. 7. Part 6: Reference 2.

(2) Chukwu, R.; Hunter, A. D.; Santarsiero, B. D. *Organometallics* **1991**, *10*, 2141–2152.

(3) Taken in part from: Chukwu, R. M.Sc. Thesis, The University of Alberta, 1990.

(4) Parts of this work have been presented orally; see ref 5 and 6.

(5) Chukwu, R.; Hunter, A. D. 73rd Canadian Chemical Conference, Halifax, Nova Scotia, July 1990; Abstract 623IN-F14.

(6) Hunter, A. D.; Chukwu, R.; Mozol, V.; Ristic-Petrovic, D. 200th National Meeting of the American Chemical Society, Washington, D.C., Aug 1990; Abstract INOR 121.

(7) See, for example: (a) Carter, F. L. *Molecular Electronic Devices*; Marcel Dekker: New York, 1982. (b) Carter, F. L. *Molecular Electronic Devices II*; Marcel Dekker: New York, 1987. (c) Mort, J.; Pfister, G. *Electronic Properties of Polymers*; Wiley: New York, 1982.

(8) See, for example: (a) Mikkelsen, K. V.; Ratner, M. A. *Chem. Rev.* **1987**, *87*, 113–153. (b) Keppeler, U.; Schnieder, O.; Stöffer, W.; Hannack, M. *Tetrahedron Lett.* **1984**, *25*, 3679–3682. (c) Metz, J.; Schnieder, O.; Hannack, M. *Inorg. Chem.* **1984**, *23*, 1065–1071. (d) Schmeder, D.; Metz, J.; Hannack, M. *Mol. Cryst. Liq. Cryst.* **1982**, *81*, 273–284. (e) Datz, A.; Metz, J.; Schneider, O.; Hannack, M. *Synth. Met.* **1984**, *9*, 31–40. (f) Metz, J.; Hannack, M. *J. Am. Chem. Soc.* **1983**, *105*, 828–830. (g) Meyer, T. J. *Prog. Inorg. Chem.* **1975**, *19*, 1–50. (h) Vergamini, P. J.; Kubas, G. J. *Prog. Inorg. Chem.* **1976**, *21*, 261–282. (i) Lemoine, P. *Coord. Chem. Rev.* **1982**, *47*, 55–88. (j) Geiger, W. E.; Connelly, N. G. *Adv. Organomet. Chem.* **1985**, *24*, 87–130.

(9) See, for example: (a) Jutzi, P.; Siemeling, U.; Müller, A.; Bögge, H. *Organometallics* **1989**, *8*, 1744–1750. (b) Lockmeyer, J. R.; Rauchfuss, T. B.; Rheingold, A. L. *J. Am. Chem. Soc.* **1989**, *111*, 5733–5738. (c) Woitellier, S.; Launay, J. P.; Spangler, C. W. *Inorg. Chem.* **1989**, *28*, 758–762. (d) Bowyer, W. J.; Geiger, W. E.; Boekelheide, V. *Organometallics* **1984**, *3*, 1079–1086. (e) Richardson, D. E.; Taube, H. *Inorg. Chem.* **1981**, *20*, 1278–1285. (f) Grentz, C.; Taube, H. *J. Am. Chem. Soc.* **1973**, *95*, 1086–1094.

0276-7333/92/2311-0589$03.00/0

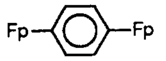

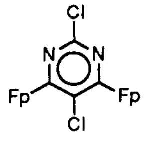

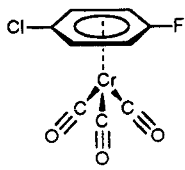

(where Fp = $(\eta^5\text{-}C_5H_5)Fe(CO)_2$), which serve as models for the analogous organometallic polymers.[2,5,6,10–13] The electrochemical oxidation behavior of these azine and bimetallic arene complexes of Fp has not been previously reported. We have therefore extended our synthetic and spectroscopic studies, and in this paper, the complete results of our electrochemical characterization of a series of halogen-substituted mono- and bimetallic arene and azine complexes of Fp are presented. In addition, the X-ray crystal structures of three of these complexes are reported and compared. The results of these studies are then used to establish how such aromatic bridging groups compare as electronic bridges to other more well-studied bridging groups such as pyrazine[14] and to establish the dependence of the magnitude of the metal–metal interactions in these species as a function of the geometry and electron richness of the aromatic bridges.

Experimental Section

Unless otherwise noted, all reactions and subsequent manipulations were performed under anaerobic and anhydrous conditions. Reagents and chemicals used were handled by conventional techniques.[15] General procedures routinely employed in the synthetic and spectroscopic studies have been described in detail previously.[2] Fp_2, FpCl, and FpI (where Fp = $CpFe(CO)_2$) used in these syntheses were prepared and purified by standard procedures.[16] The arene complexes $1,4\text{-}C_6H_4Fp_2$ (**1**),[11b] $1,3\text{-}C_6H_4Fp_2$ (**2**),[11b] $1,4\text{-}C_6F_4Fp_2$ (**3**),[11b] $1,3\text{-}C_6F_4Fp_2$ (**4**),[11b,17a] C_6H_5Fp (**5**),[17] and C_6F_5Fp (**6**)[17] were prepared by the literature methods as were the azine complexes **10–18**.[2] Synthetic procedures and nonoptimized yields for the new complexes **7–9** and **19** and their analytical, mass spectral, and IR data are recorded below.

Synthesis of $1,2,3,5\text{-}C_6H_2F_3Fp$ (8). The synthesis of this compound was carried out by a procedure analogous to that described in the literature.[18] Thus, to a solution of NaFp (13.3 mmol) in THF (70 mL), prepared as described previously,[2] was added $1,2,3,5\text{-}C_6H_2F_4$ (2.00 g, 13.3 mmol) at ~ −78 °C, and the solution was stirred at this temperature for about 1 h. The cooling source was then removed, and the solution was stirred for a further 2 h, during which time its contents were warmed to ambient temperature. The solution was then taken to dryness in vacuo, and the product was isolated as the second band from a chromatography column packed with Florisil and with pentane as eluent. The product was crystallized from CH_2Cl_2 (~10 mL) to give a 48% yield (1.96 g, 6.37 mmol) of $1,2,3,5\text{-}C_6H_2F_3Fp$ (**8**) as a yellow powder. Anal. Calcd for **8**, $C_{13}H_7F_3FeO_2$: C, 50.69; H, 2.29. Found: C, 50.48; H, 2.29. IR (CH_2Cl_2): ν_{CO} 2040 (s), 1982 (s) cm^{-1}. Low-resolution mass spectrum: m/z 308 (P^+). $^{19}F\{^1H\}$ NMR ($(CD_3)_2SO$): −112.1 (dd, F2, $J_{2,3}$ = 30 Hz, $J_{2,5}$ = 16 Hz), −119.5 (dd, F5, $J_{3,5}$ = 1.5 Hz), −135.9 (dd, F3) ppm.

Syntheses of $1,3\text{-}C_6F_4Fp_2$ (4), $1,4\text{-}C_6H_4FFp$ (7), and $1,2,3,4,6\text{-}C_6HF_4Fp$ (9). These compounds were synthesized in a similar manner, the synthesis of $1,4\text{-}C_6H_4FFp$ being described in detail as a representative example.

In a 300-mL three-neck flask fitted with an addition funnel was placed *n*-BuLi (2.5 M solution in hexane, 2 mL, 5.0 mmol) followed by an Et_2O/hexane (50:50) mixture (40 mL). The solution was cooled to ~−78 °C. The compound $1,4\text{-}C_6H_4FBr$ (2.00 g, 11.4 mmol) was placed in the addition funnel, and Et_2O (20 mL) was added. This solution was added to the cold mixture in the flask over a period of 10 min. The cooling source was removed, the mixture was warmed to room temperature and it was then stirred for an additional 20 min at 10–15 °C. The mixture was again cooled to ~−78 °C, and THF (50 mL) was added. To the resulting greenish solution was added solid FpI (3.47 g, 11.4 mmol) over 5 min. The mixture was then stirred at ~−78 °C for 1 h, and the cooling source was removed. After 2 h, the solution was taken to dryness in vacuo and the resulting solid dissolved in heptane/toluene (50:50, 15 mL). This solution was chromatographed on a Florisil-packed (14 × 5 cm) column with pentane as eluent. The first bright yellow band eluted had carbonyl bands in the IR region at 2003 (vs) and 1942 (vs) cm^{-1} (in CH_2Cl_2). The compound was identified by mass spectroscopy to be FpBu ($C_{11}H_{14}FeO_2$, m/z 234, P^+) but was not further studied. The second yellow band contained the desired product and was taken to dryness to give a 63% yield (1.90 g, 7.0 mmol) of the desired product, $1,4\text{-}C_6H_4FFp$ (**7**), as a bright yellow powder. Anal. Calcd for **7**, $C_{13}H_9FFeO_2$: C, 57.39; H, 3.33. Found: C, 57.44; H, 3.87. IR (CH_2Cl_2): ν_{CO} 2020 (s), 1965 (s) cm^{-1}. Low-resolution mass spectrum: m/z 272 (P^+). ^1H NMR ($(CD_3)_2SO$): 5.2 (s, 5 H, C_5H_5), 6.8 (m, 2 H, $C_6(H_A)_2(H_B)_2FFp$), 7.3 (m, 2 H, $C_6(H_A)_2(H_B)_2FFp$) ppm. ^{19}F NMR ($(CD_3)_2SO$): −124.04 (m, F4) ppm.

Compounds **4** and **9** ($1,3\text{-}C_6F_4Fp_2$ and $1,2,3,4,6\text{-}C_6HF_4Fp$, respectively) were synthesized from $1,3\text{-}C_6H_2F_4$ in an analogous manner (using 2 and 1 equiv of BuLi, respectively) in yields of 8 and 55%, respectively. Alternately, **4** could be prepared from **9**, using the method described above, in 68% yield (37% from $1,3\text{-}C_6H_2F_4$). Anal. Calcd for **4**, $C_{20}H_{10}F_4Fe_2O_4$: C, 47.85; H, 2.01. Found: C, 47.66; H, 2.20. IR (CH_2Cl_2): ν_{CO} 2028 (s), 1981 (s) cm^{-1}.

---

(10) The azine complexes include various pyridine, pyrazine, pyridazine, and pyrimidine species in which the Fp groups are attached to the azine rings by Fe–C σ bonds.

(11) (a) Hunter, A. D. *Organometallics* **1989**, *8*, 1118–1120. (b) Hunter, A. D.; Szigety, A. B. *Organometallics* **1989**, *8*, 2670–2679. (c) Hunter, A. D.; McLernon, J. L. *Organometallics* **1989**, *8*, 2679–2688.

(12) (a) Richter-Addo, G. B.; Hunter, A. D. *Inorg. Chem.* **1989**, *28*, 4063–4065. (b) Richter-Addo, G. B.; Hunter, A. D.; Wichrowska, N. *Can. J. Chem.* **1989**, 41–48.

(13) The electrochemical behavior of some related monometallic derivatives of Fp has been reported previously; see: (a) Tracey, A. A.; Eriks, K.; Prock, A.; Giering, W. P. *Organometallics* **1990**, *9*, 1399–1405. (b) Tilset, M.; Parker, V. D. *J. Am. Chem. Soc.* **1989**, *111*, 6711–6717. (c) Zhen, Y.; Feighery, W. G.; Lai, C.-K.; Atwood, J. D. *J. Am. Chem. Soc.* **1989**, *111*, 7832–7837. (d) Liu, H.-Y.; Golovin, M. N.; Fertal, D. A.; Tracey, A. A.; Eriks, K.; Giering, W. P.; Prock, A. *Organometallics* **1989**, *8*, 1454–1458. (e) Philp, R. H.; Reger, D. L.; Bond, A. M. *Organometallics* **1989**, *8*, 1714–1718. (f) Legzdins, P.; Wassink, B.; Einstein, F. W. B.; Jones, R. H. *Organometallics* **1988**, *7*, 477–481. (g) Golovin, M. N.; Meirrowitz, R.; Rahman, M. M.; Liu, H. Y.; Prock, A.; Giering, W. P. *Organometallics* **1987**, *6*, 2285–2289. (h) Bitcon, C.; Whiteley, M. W. *J. Organomet. Chem.* **1987**, *336*, 385–392. (i) Joseph, M. F.; Page, J. A.; Baird, M. C. *Inorg. Chim. Acta* **1982**, *64*, L121–L122. (j) Magnuson, R. H.; Zulu, S.; T'sai, W.-M.; Giering, W. P. *J. Am. Chem. Soc.* **1980**, *102*, 6887–6888. (k) Klingler, R. J.; Kochi, J. K. *J. Organomet. Chem.* **1980**, *202*, 49–63. (l) Rogers, W.; Page, J. A.; Baird, M. C. *J. Organomet. Chem.* **1978**, *156*, C37–C42. (m) Slack, D. A.; Baird, M. C. *J. Am. Chem. Soc.* **1976**, *98*, 5539–5546. (n) Legzdins, P.; Wassink, B. *Organometallics* **1984**, *3*, 1811–1817.

(14) Similar cyclic voltammetric studies have been reported for other bimetallic complexes whose bridging ligands have an aromatic core. See for example, ref 9c and: (a) Felix, F.; Ludi, A. *Inorg. Chem.* **1978**, *17*, 1782–1782. (b) Order, N. V.; Geiger, W. E.; Bitterwolf, T. E.; Rheingold, A. L. *J. Am. CHem. Soc.* **1987**, *109*, 5680–5690. (c) Cayton, R. H.; Chisholm, M. H. *J. Am. Chem. Soc.* **1989**, *111*, 8921–8923. (d) Rommel, J. S.; Weinrach, J. B.; Grubisha, D. S.; Bennett, D. W. *Inorg. Chem.* **1988**, *27*, 2945–2949. (e) Kobel, W.; Hanack, M. *Inorg. Chem.* **1986**, *25*, 103–107. (f) Gross, R.; Kaim, W. *Inorg. Chem.* **1986**, *25*, 498–506. (g) Zulu, M. M.; Lees, A. J. *Inorg. Chem.* **1988**, *27*, 1139–1145. (h) Lay, P. A.; Magnuson, R. H.; Taube, H. *Inorg. Chem.* **1988**, *27*, 2364–2371. (i) Zulu, M. M.; Lees, A. J. *Organometallics* **1989**, *8*, 955–960. (j) Zulu, M. M.; Lees, A. J. *Inorg. Chem.* **1989**, *28*, 85–89. (k) Albinati, A.; Isaia, F.; Kaufmann, W.; Sorato, C.; Venanzi, L. M. *Inorg. Chem.* **1989**, *28*, 1112–1122. (l) Ernst, S. D.; Kaim, W. *Inorg. Chem.* **1989**, *28*, 1520–1528.

(15) (a) Perrin, D. D.; Armarego, W. L. F.; Perrin, D. R. *Purification of Laboratory Chemicals*, 3rd ed.; Pergamon: New York, 1987. (b) Shriver, D. F.; Drezdzon, M. A. *The Manipulation of Air Sensitive Compounds* 2nd ed.; Wiley: New York, 1986.

(16) (a) King, R. B.; Eisch, J. J. *Organomet. Synth.* **1965**, *1*, 114. (b) *Ibid.*, **1965**, *1*, 151.

(17) (a) Cohen, S. C. *J. Chem. Soc., Dalton Trans* **1973**, 553–555. (b) Piper, T. S.; Wilkinson, G. *J. Inorg. Nucl. Chem.* **1956**, *3*, 104–124. (c) Artamkina, G. A.; Milchenko, A. Y.; Beletskaya, I. P.; Reutov, O. A. *J. Organomet. Chem.* **1986**, *311*, 199–206.

(18) See, for example: (a) Bruce, M. I.; Stone, F. G. A. *J. Chem. Soc. A* **1966**, 1837–1842. (b) Bruce, M. I. *J. Organomet. Chem.* **1967**, *10*, 495–504. (c) Bruce, M. I. *J. Organomet. Chem.* **1970**, *21*, 415–425. (d) King, R. B.; Bisnette, M. B. *J. Organomet. Chem.* **1964**, *2*, 38–43.

Table I. Cyclic Voltammetry Data for the Oxidations of the Complexes in CH_2Cl_2[a]

compd formula[b,c]	compd no.	scan rate, V s^{-1}	$E°'$,[d] V	ΔE, V	$i_{p,c}/i_{p,a}$
1,4-$C_6F_4Fp_2$	3	0.1	1.35, *e*	0.07, *e*	0.78, *e*
		1.0	1.35, *e*	0.09, *e*	0.97, *e*
		5.0	1.35, 1.63	0.10, 0.12	0.97, 0.88
1,3-$C_6F_4Fp_2$	4	1.0	1.36, 1.59	0.09, 0.14	0.74, 0.55
		5.0	1.36, 1.58	0.12, 0.15	0.80, 0.71
C_6F_5Fp	6	0.1	1.64	0.110	0.65
		1.0	1.64	0.130	0.81
1,2,3,4,6-C_6HF_4Fp[c]	9	0.1	1.56	0.090	0.61
		2.0	1.56	0.130	0.83
C_5NF_4Fp[c]	10	0.1	1.76	0.08	0.86
		1.0	1.76	0.10	0.98
C_5NClF_3Fp[c]	11	0.1	1.71	0.08	0.85
		1.0	1.72	0.11	0.99
$C_5NCl_2F_2$-Fp[c]	12	0.1	1.66	0.09	0.94
		1.0	1.66	0.10	0.97

[a] In 0.1 M [n-Bu_4N]PF_6 at a Pt-bead electrode. [b] Where Fp ≡ (η^5-C_5H_5)Fe(CO)$_2$. [c] The isomeric identities of these complexes are given in Figure 1. [d] Formal oxidation potentials, $E°'$, are measured vs the SCE, for which the ferrocene couple is observed at +0.47 V. [e] At this scan rate this oxidation gives rise to an adsorption wave (see text).

Low-resolution mass spectrum: m/z 502 (P^+). ^{19}F NMR (($(CD_3)_2SO$): −45.3 (d, F2, $J_{2,5}$ = 12 Hz), −108.1 (d, F4/F6, $J_{4/6,5}$ = 29 Hz), −166.0 (dt, F5) ppm. Anal. Calcd for **9**, $C_{13}H_6F_4FeO_2$: C, 48.78; H, 1.88. Found: C, 48.24; H, 2.05. IR (CH_2Cl_2): ν_{CO} 2037 (s), 1986 (s) cm^{-1}. Low-resolution mass spectrum: m/z 326 (P^+). ^{19}F NMR ($(CD_3)_2SO$): −81.2 (m, F6), −100.3 (m, F2), −141.6 (m, F4), −167.6 (m, F3) ppm.

Electrochemical Analysis of the Products. The electrochemical analyses were carried out using the equipment and experimental methods described in detail previously.[11e] Thus, the working electrode was a small (~1 mm diameter) Pt bead sealed in soft glass. An aqueous SCE reference electrode was used and was separated from the working electrode compartment by a fine frit and a Luggin probe. The support electrolyte, [n-Bu_4N]PF_6, and the cell parts were dried in an oven at 130 °C overnight just prior to use. Dichloromethane (Spectrograde, BDH) was used for the solvent and was first stirred over alumina (5 g, Woelm neutral, W200 Super 1) while simultaneously being purged with prepurified dinitrogen for 30 min. The solvent with some entrained alumina (~0.5 g) was then transferred by cannula to the electrochemical cell, which had been previously set up on a vaccum line under argon. The solutions employed during cyclic voltammetry were typically (5–7) × 10^{-4} M in organometallic complex and 0.1 M in [n-Bu_4N]PF_6.

The potentials were generated by a BAS CV27 voltammograph, and the resulting cyclic voltammograms were recorded on a Hewlett-Packard 7090A X-Y recorder. The formal oxidation potential, $E°'$, for reversible couples is defined as the average of the anodic ($E_{p,a}$) and cathodic ($E_{p,c}$) peak potentials. The separation of the cathodic and anodic potentials ΔE is defined by $|E_{p,c}-E_{p,a}|$, and the cathodic to anodic peak current ratio is defined by $i_{p,c}/i_{p,a}$.[19] Diffusion control was established for redox processes by the observation of a linear plot of $i_{p,c}$ vs the square root of scan rate ($v^{1/2}$) over at least 1 order of magnitude of scan rate. The oxidation of ferrocene is reported to be highly reversible in many solvents.[20a] After each experiment, ferrocene was added as an internal reference.[20b] Under our experimental conditions, ferrocene is reversibly oxidized ($E°'$ = +0.47 V vs SCE, $i_{p,c}/i_{p,a}$ = 1.0, ΔE = 60–70 mV, 0.1 V s^{-1}). The ratio $i_{p,c}/i_{p,a}$ is used throughout the text to establish chemical reversibility for the complexes studied. The electrochemical reversibility was established by comparison of the scan rate dependence of ΔE of the analyte to that of ferrocene recorded under identical conditions. The oxidation waves were established to be one electron in nature by comparison of anodic–cathodic peak potential separations and peak currents at a variety of scan rates (0.1–10.0 V s^{-1}) to those of ferrocene recorded under identical conditions.[20b] In general, reversible first oxidations were exhausted before the second oxidations were studied, usually with a fresh electrode.

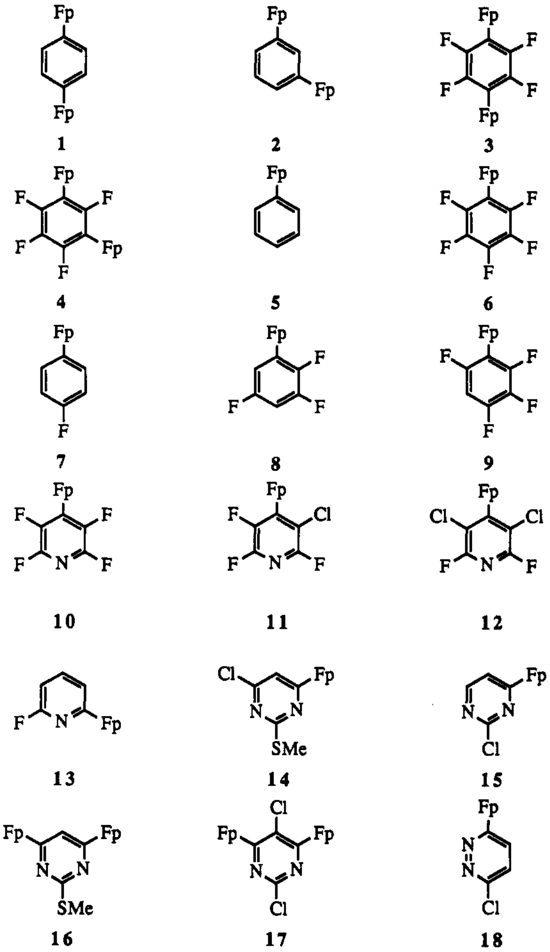

Figure 1. Isomeric forms of the complexes.

Eleven of the complexes studied displayed only chemically irreversible oxidations at the moderate scan rates employed. At 0.1 V s^{-1} their anodic peak potentials, $E_{p,a}$, were observed at 0.90 (**1**), 1.09 (**2**), 1.16 (**5**), 1.22 (**7**), 1.54 (**8**), 1.25 (**13**), 1.40 (**14**), 1.42 (**15**), 1.06 (**16**), 1.18 (**17**), and 1.40 (**18**) V. Electrochemical data for the seven complexes displaying chemically reversible behavior at these scan rates are collected in Table I.

X-ray Crystal Structure Determinations for Complexes $C_{20}H_{10}F_4Fe_2O_4$ (3), $C_{13}H_5F_5FeO_2$ (6), and $C_{12}H_5F_4FeNO_2$ (10). Crystal suitable for X-ray examination were mounted on glass fibers and optically centered in the X-ray beam on an Enraf-Nonius CAD4 automated diffractometer. Data collection and structure solution parameters are given in Table II. Data were corrected for Lorentz and polarization effects and also for absorption (via the method of Walker and Stuart for **3** and **6**[21f] and via empirical ψ scans for **10**). Details of the usual procedures in our laboratories have been published elsewhere.[2,22a] Structure

---

(19) Nicholson, R. S. *Anal. Chem.* **1966**, *38*, 1406.

(20) (a) Holloway, J. D. L.; Geiger, W. E. *J. Am. Chem. Soc.* **1980**, *101*, 2038–2044. (b) Gagne, R. R.; Koval, C. A.; Lisensky, G. C. *Inorg. Chem.* **1980**, *19*, 2854–2855.

(21) (a) The diffractometer programs are those supplied by Enraf-Nonius for operating the CAD4F diffractometer, with some local modifications Dr. R. G. Ball. (b) *International Tables for X-ray Crystallography*; Kynoch Press: Birmingham, U.K., 1974; Vol. I. (c) The computer programs used in this analysis include the Enraf-Nonius Structure Determinations Package, Version *3*, 1985, Delft, The Netherlands, adapted for a SUN Microsystems 3/160 computer, and several locally written programs by Dr. R. G. Ball. (d) *International Tables for X-ray Crystallography*; Kynoch Press: Birmingham, U.K., 1974; Vol. IX, Table 2.2B (present distributor D. Reidel, Dordrecht, The Netherlands). (e) *Ibid.*, Table 2.3.1. (f) Walker, N.; Stuart, D. *Acta Crystallogr.* **1983**, *A39*, 158.

(22) (a) Holton, J.; Lappert, M. F.; Ballard, D. G. H.; Pearce, R.; Atwood, J. L.; Hunter, W. E. *J. Chem. Soc., Dalton Trans.* **1979**, 45. (b) Sheldrick, G. M. In *Crystallographic Computing 3*; Sheldrick, G. M., Kruger, C., Goddard, R., Eds.; Oxford University Press: London, 1985; pp 175–189. (c) Sheldrick, G. M. Shelx-a System of Computer Programs for X-Ray Structure Determination; Cambridge University: Cambridge, England, 1976.

Table II. Summary of Crystal Data and Intensity Collection for the Complexes

param	3	6	10
formula	$C_{20}H_{10}F_4Fe_2O_4$	$C_{13}H_5F_5FeO_2$	$C_{12}H_5F_4FeNO_2$
fw	501.98	344.02	327.03
cryst dimens, mm	0.099 × 0.167 × 0.182	0.262 × 0.258 × 0.528	0.21 × 0.15 × 0.08
space group	$P2_1/c$	*Pnma*	*Pnma*
cryst syst	monoclinic	orthorhombic	orthorhombic
a, Å	7.714 (1)	6.993 (2)	6.948 (1)
b, Å	9.840 (1)	12.774 (4)	12.828 (1)
c, Å	12.473 (1)	13.649 (3)	13.000 (1)
β, deg	107.822 (7)		
V, $Å^3$	901.3	1219.2	1159
Z	2	4	4
calcd density, g cm^{-3}	1.850	1.771	1.881
abs coeff, cm^{-1}	16.73	12.80	12.82
diffractometer	Enraf-Nonius CAD4	Enraf-Nonius CAD4	Enraf-Nonius CAD4
radiation	Mo Kα (λ = 0.7107 Å)	Mo Kα (λ = 0.7107 Å)	Mo Kα (λ = 0.7107 Å)
monochromator/filter	incident beam, graphite cryst	Zr filter	incident beam, graphite cryst
takeoff angle, deg	3.00	3.00	2.8
detector aperture, mm	2.40 (horiz) × 4.0 (vert)	2.40 (horiz) × 4.0 (vert)	3.00 + tan θ (horiz) × 4.0 (vert)
cryst to detector dist, mm	205	205	205
scan type	ω–2θ	θ–2θ	θ–2θ
scan width	0.500 + 0.347 tan θ	0.500 + 0.347 tan θ	0.80 + 0.35 tan θ
scan rate, deg min^{-1}	1.0–4.0	2.0	0.8–8.0
2θ range, deg	2–60	2–56	2–50
data collection index range	$h,\pm k,\pm l$	$\pm h,k,\pm l$	hkl
no. of rflns	2637 total, averaged	1721 total, averaged	1254 total
no. of signif rflns	1309 ($I > 3\sigma_I$)	1097 ($I > 3\sigma_I$)	798 ($I > 3\sigma_I$)
observns/variables ratio	1309/136	1097/103	798/97
agreement factor R_1, R_2, GOF	0.039, 0.044, 1.25	0.037, 0.047, 1.64	0.0308, 0.0315, 1.07
cor applied	empirical abs cor	empirical abs cor	ψ scans

Table III. Atomic Coordinates and Equivalent Isotropic Displacement Parameters for Complex 3[a,b]

atom	*x*	*y*	*z*	U_{eq}
Fe	2733.6 (7)	1806.9 (6)	2270.9 (4)	40.0 (1)
F1	−1158 (3)	2465 (2)	460 (2)	59 (1)
C1	−514 (4)	1220 (4)	263 (3)	39 (1)
C2	1168 (4)	782 (4)	937 (3)	38 (1)
C3	1596 (4)	−486 (4)	625 (3)	39 (1)
F3	3200 (3)	−1078 (2)	1237 (2)	65 (1)
C4	2377 (5)	3364 (4)	1541 (3)	48 (1)
O4	2207 (4)	4392 (3)	1084 (2)	67 (1)
C5	4707 (5)	1476 (4)	1903 (3)	50 (1)
O5	6033 (4)	1298 (4)	1677 (3)	76 (1)
C6	3145 (6)	438 (5)	3607 (3)	68 (1)
C7	4093 (6)	1635 (5)	3989 (3)	70 (1)
C8	2830 (7)	2692 (5)	3802 (3)	74 (1)
C9	1077 (6)	2127 (6)	3300 (3)	76 (1)
C10	1316 (6)	750 (5)	3209 (3)	73 (1)

[a] Atomic coordinates ×10^4 and U_{eq}'s ×10^3 $Å^2$. [b] The equivalent isotropic Gaussian displacement parameter U_{eq} is $^1/_3\sum_{i=1}^{3} r_i^2$, where r_i values are the root-mean-square amplitudes of the anisotropic Gaussian diaplacement parameters.

Table IV. Atomic Coordinates and Equivalent Isotropic Displacement Parameters for Complex 6[a]

atom	*x*	*y*	*z*	U_{eq}
Fe	4687.2 (8)	2500	4366.1 (4)	26.1 (1)
C1	4976 (5)	2500	5820 (3)	25 (1)
C2	5107 (4)	1595 (2)	6377 (2)	34 (1)
C3	5310 (4)	1582 (3)	7383 (2)	44 (1)
C4	5390 (6)	2500	7890 (3)	44 (1)
C5	2922 (4)	1506 (2)	4407 (2)	34 (1)
O5	1759 (3)	880 (2)	4394 (2)	50 (1)
C6	7681 (6)	2500	4292 (3)	51 (1)
C7	6968 (5)	1618 (3)	3825 (3)	60 (1)
C8	5837 (5)	1977 (4)	3053 (2)	85 (1)
F2	5024 (3)	647 (1)	5928 (1)	54 (1)
F3	5400 (3)	661 (2)	7868 (1)	73 (1)
F4	5541 (4)	2500	8868 (2)	66 (1)

[a] Atomic coordinates ×10^4 and U_{eq}'s ×10^3 $Å^2$.

Table V. Atomic Coordinates and Equivalent Isotropic Displacement Parameters for Complex 10[a]

atom	*x*	*y*	*z*	U_{eq}
Fe	4795 (1)	2500	4476.4 (5)	35 (5)
F2	5055 (5)	4343 (2)	6138 (2)	74 (25)
F3	5310 (5)	4251 (2)	8174 (2)	103 (23)
O	1864 (4)	884 (2)	4468 (3)	69 (14)
C	3011 (5)	1506 (3)	4494 (3)	48 (7)
C1	5000 (7)	2500	5988 (3)	37 (8)
C2	5102 (6)	3392 (3)	6588 (3)	46 (3)
C3	5235 (6)	3351 (3)	7638 (3)	60 (16)
N	5298 (7)	2500	8182 (4)	65 (29)
C11	7815 (7)	2500	4465 (4)	49 (17)
C12	7141 (6)	1620 (4)	3955 (3)	62 (11)
C13	6042 (6)	1967 (4)	3122 (3)	80 (38)

[a] Atomic coordinates ×10^4 and U_{eq}'s ×10^3 $Å^2$.

Table VI. Selected Bond Lengths and Angles for Complexes 3, 6, and 10

bond length or angle[a]	3	6	10
Fe–C(aromatic)	2.004 (3)	1.994 (3)	1.970 (4)
Fe–C(carbonyl)	1.761 (4), 1.749 (4)	1.772 (3)	1.779 (4)
Fe–Cp(centroid)	1.722	1.722	1.723
C–O	1.148 (5), 1.155 (4)	1.140 (3)	1.128 (4)
Cp–Fe–C(aromatic)	119.7	121.0	120.5
Cp–Fe–C(carbonyl)	125.8, 125.1	125.2	125.5
C(carbonyl)–Fe–C(carbonyl)	92.1 (2)	91.56 (11)	91.6 (2)
C(carbonyl)–Fe–C(aromatic)	92.8 (2), 92.3 (2)	92.24 (10)	92.2 (2)

[a] Bond lengths are in Å; bond angles are in deg.

solution proceeded in a routine fashion for all three compounds with the SDP structure solution package[21a,c] for compounds 3 and 6 and SHELXS-86[22b] and SHELX-76[22c] for 10. All non-hydrogen atoms were treated with anisotropic thermal parameters, and all hydrogen atoms were geometrically generated and included in the model as "riding" on the attached atom with isotropic thermal parameters constrained to be 1.2 times those of the attached atom. Final fractional atomic coordinates and equivalent isotropic thermal parameters are given in Tables III–V for compounds 3, 6, and 10, respectively. Selected bond lengths and angles for complexes 3, 6, and 10 are given in Table VI.

Results and Discussion

Most of the mono- and bimetallic aryl and azinyl complexes of Fp (where Fp = (η^5-C_5H_5)Fe(CO_2) required for this work (i.e. compounds 1–3, 5, 6, 10–18; see Figure 1) were prepared as described in detail previously.[2,11b] The remaining four complexes were prepared by analogous methods. Thus, metathesis between NaFp and 1,2,3,5-$C_6H_2F_4$ produces complex **8**; e.g.

$$1,2,3,5\text{-}C_6H_2F_4 + NaFp \rightarrow 1,2,3,5\text{-}C_6H_2F_3Fp + NaF \quad (1)$$

while metathesis between FpI and an aryllithium reagent, e.g.

$$1,4\text{-}C_6H_4FLi + FpI \rightarrow 1,4\text{-}C_6H_4FFp + NaF \quad (2)$$

produced complexes **4**, **7**, and **9**. Each complex was synthesized via the most direct route from convenient commercial starting materials, and no attempt was made to optimize the yields of 8, 63, 48, and 55% for complexes **4**, **7**, **8**, and **9**, respectively. These reactions also generally produced other organometallic products in addition to those desired. Thus, in the synthesis of **4**, i.e.

$$C_6H_2F_4 \xrightarrow[\text{(2) 2FpI, −78 °C}]{\text{(1) excess } n\text{-BuLi, THF}} 1,3\text{-}C_6F_4Fp_2 + C_6HF_4Fp + BuFp + Fp_2 \quad (3)$$

one observes a complex mixture of materials which includes the ubiquitous Fp_2 dimer (formed by reduction of FpI),[2,11] C_6HF_4Fp (which arises from incomplete deprotonation of the starting arene),[23] and BuFp (due to the presence of excess BuLi). Thus, difficulty in the purification of complex **4** from the reaction mixture partially accounts for the relatively low isolated yield of **4**. The overall yield of **4** could be substantially improved, from 8 to 37%, by preparing it from **9**, i.e.

$$1,2,3,4,6\text{-}C_6HF_4Fp \xrightarrow[\text{(2) FpI, −78 °C}]{\text{(1) } n\text{-BuLi, THF}} 1,3\text{-}C_6F_4Fp_2 \quad (4)$$

The identity of each of these new products (Figure 1) was established by its analytical and spectroscopic properties. Of particular utility were their ^{19}F NMR spectra,[24] which unambiguously established their structures.[25] As expected, increasing the number of electron-withdrawing fluorine substituents on the aryl ligands in the complexes $C_6H_{5-n}F_nFp$ results in a steady increase in the carbonyl stretching frequencies for both symmetric and antisymmetric stretching frequencies (i.e., from 2016 (s) and 1962 (s) cm^{-1} for compound **5**, C_6H_5Fp, to 2038 (s) and 1989 (s) cm^{-1} for compound **6**, C_6F_5Fp). This correlation reflects the reduced electron density at the metal center on the fluorinated complexes and indicates facile electronic interaction between the metal center and the arene ring.[26]

Electrochemical Characterization of the Complexes. The oxidative behavior for the 18 complexes were studied by cyclic voltammetry in CH_2Cl_2; e.g.

$$C_5NF_4Fp \underset{+e^-}{\overset{-e^-}{\rightleftharpoons}} [C_5NF_4Fp]^{\bullet+} \quad (5)$$

and the results are summarized in Table I for those complexes displaying chemically reversible oxidation behavior (i.e. **3**, **4**, **6**, **9**, **10**, **11**, and **12**) at the moderate scan rates employed (i.e. 0.01–1.0 V s^{-1}). It is generally accepted that the electrons removed in the oxidations of Fp–X compounds are located in orbitals which are primarily metal centered.[13,27] Decreasing the electron density on an arene ring is expected to result in the stabilization of the arene orbitals and consequently the stabilization of the highest occupied molecular orbitals, HOMO, of the complex[27] from which the oxidation takes place. Thus, we were not surprised to observe that the ease of oxidation of these complexes was dependent on the number of electron-withdrawing groups on the arene ring. For example, IR spectral data indicate[2] that fluorine substitution in the complexes 4-C_5NX_4Fp produces a more electron-poor aromatic ring than does chlorine substitution. This results in complex **10** (C_5NF_4Fp) being observed to be more electron poor than complex **11** (C_5NF_3ClFp), which is, in turn, observed to be more electron poor than complex **12** ($C_5NF_2Cl_2Fp$) on the basis of the carbonyl stretching frequencies.[28] Thus, we were not surprised that those complexes with the greatest number of fluorine substituents were oxidized with the most difficulty (e.g. for complexes **10**, **11**, and **12** the $E^{\circ\prime}$ values were 1.76, 1.71, and 1.66 V, respectively, at 0.1 V s^{-1}). Indeed, the replacement of each chloro by a fluoro substituent increased the oxidation potential by 50 mV. Similarly, the introduction of an aza (N) group on the aromatic ring would be expected to polarize the electron distribution about the aromatic ring and to inductively reduce the electron density of the aromatic carbons. Thus, decreases in the electron density and increases in the oxidation potentials of the Fp groups are expected. In our studies, this increase amounts to about 200 mV per aza group (e.g. compound **9**, 1,2,3,4,6-C_6HF_4Fp, has an $E^{\circ\prime}$ value of 1.56 V, whereas compound **10**, C_5NF_4Fp, has an $E^{\circ\prime}$ value of 1.76 V). These observations are consistent with the spectroscopic data[2] and indicate increased metal to arene electron transfer with decreasing electron richness of the aromatic ring.

The degree of chemical reversibility of the oxidations exhibited by compounds of this type is primarily dependent upon the stability of the oxidized forms. We observe that increasing the number of electron-withdrawing F groups on the phenyl or pyridyl ring generally results in an increase in the degree of chemical reversibility for related series of compounds. Thus, all of the mono-Fp-substituted aryl or azinyl complexes with four or more F or Cl groups exhibit moderate to excellent chemical reversibilities (i.e. $i_{p,c}/i_{p,a} \geq 0.60$ at 0.1 V s^{-1}, see Table I), whereas all other complexes with three or less halogen substituents showed complete chemical irreversibility (i.e., no return peaks were observed after their oxidations at similar scan rates). Furthermore, introduction of an aza group (N) para to the carbon atom bearing the organometallic substituent also resulted in a substantial increase in the degree of reversibility for related complexes (e.g. $i_{p,c}/i_{p,a} = 0.65$ and 0.86 for C_6F_5Fp and C_5NF_4Fp at 100 mV $s1^{-1}$). These results demonstrate that, for those complexes with fewer electron-withdrawing groups on the aromatic ring, the radical cation produced upon oxidation is more rapidly decomposed, i.e.

$$Fp\text{–}Ar \underset{+e^-,\,k_2}{\overset{-e^-,\,k_1}{\rightleftharpoons}} [Fp\text{–}Ar]^{\bullet+} \xrightarrow{k_3} \text{decomposition} \quad (6)$$

(i.e. k_3 is relatively large) than it is for the more elec-

---

[23] See ref 13f and: (a) Pickett, C. J.; Pletcher, D. *J. Chem. Soc., Dalton Trans.* **1975**, 87–91. (b) Dessy, R. E.; Stary, F. E.; King, R. B.; Waldrop, M. *J. Am. Chem. Soc.* **1966**, *88*, 471. (c) Brandsma, L. *Preparative Polar Organometallic Chemistry*; Springer-Verlag: Berlin, Heidelberg, 1987; Vol. I.

[24] (a) Bruce, M. I. *J. Chem. Soc.* **1968**, 1459–1464. (b) Buckingham, A. D.; Petcher, E.; Stone, F. G. A. *J. Chem. Phys.* **1962**, *36*, 124–129.

[25] In the cases of complexes 7 and 9, whose analytical data are not entirely satisfactory, their spectroscopic data indicated that no other organometallic products were present and that these materials contained traces of the crystallization solvents as impurities.

[26] See, for example: (a) Butler, I. R.; Lindsell, W. E.; Thomas, M. J. K. *J. Organomet. Chem.* **1984**, *262*, 59–68. (b) Steward, R. P.; Treichel, P. M. *J. Am. Chem. Soc.* **1970**, *92*, 2710–2718.

[27] See, for example: Schilling, B. E. R.; Hoffmann, R.; Lichtenberger, D. L. *J. Am. Chem. Soc.* **1979**, *101*, 585–591.

[28] This effect must be inductive in nature and is due to the greater electronegativity of F over that of Cl. If it were due to π donation from the lone pairs on the halogen, the opposite trend would be expected, since F is the stronger π donor.[2]

tron-poor complexes. The substantial difference in reversibilities observed between complexes **6** and **10**, which are sterically almost identical around iron (see below), confirms the suggestion that electronic effects largely account for the differences in reversibilities observed within these series of complexes. Interestingly, all of the complexes having an aza group ortho to the carbon atom bearing the organometallic substituent (complexes **13**–**18**, Figure 1) displayed chemically irreversible oxidations under similar conditions, perhaps because of involvement of the ortho heteroatoms in the decomposition of the radical cations.[29]

Electrochemical studies on four representative arene-bridged bimetallic complexes of iron (1,4-$C_6H_4Fp_2$ (**1**), 1,3-$C_6H_4Fp_2$ (**2**), 1,4-$C_6F_4Fp_2$ (**3**), and 1,3-$C_6F_4Fp_2$ (**4**)) and on the related monometallic products (i.e. C_6H_5Fp (**5**), and C_6F_5Fp (**6**)) were carried out in the greatest detail. The spectroscopic data on these and some related complexes indicate[11b,c,27] that their iron centers are acting as both σ and π donors to the arenes, which makes their aromatic rings very electron rich.[11b,c,12] These data also suggest that the metal centers in these species interact primarily through the arenes' π systems and that these interactions are strongest for the para-substituted complexes (as they are for "organic" substituents such as NMe_2 and CN).[11b,c] In molecular orbital terms, metal to arene π donation (from essentially nonbonding filled d orbitals on iron to vacant π^* orbitals on the arene) seems to be maximal for para-substitution geometries and this may give such complexes partial metal–arene multiple-bond character, i.e.[3,4,11b]

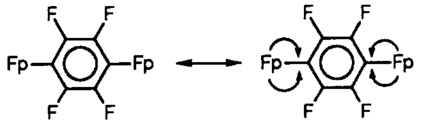

As expected,[13] cyclic voltammetry reveals that monometallic complex **5** displays only chemically irreversible electron-transfer processes at scan rates of up to 10.0 V s^{-1}; i.e.

$$C_6H_5Fp \xrightarrow{-e^-} \text{“}[C_6H_5Fp]^{\bullet+}\text{”} \xrightarrow{\text{rapid}} \text{decomposition} \qquad (7)$$

Similarly, the bimetallic perhydro complexes **1** and **2** exhibit only chemically irreversible oxidations ($E_{p,a}$ = 0.90 and 1.09 V vs SCE, respectively, at a scan rate of 0.1 V s^{-1}) at scan rates of up to 10 V s^{-1}; i.e.

$$C_6H_4Fp_2 \xrightarrow{-e^-} \text{“}[C_6H_4Fp_2]^{\bullet+}\text{”} \xrightarrow{\text{rapid}} \text{decomposition} \qquad (8)$$

Similar irreversible one-electron oxidations have been previously reported for related complexes and have been ascribed to decomposition of the radical cationic products (i.e. $[CpFe(CO)_2R]^{\bullet+}$, where R = vinyl, C_2R, etc.).[13]

Fortunately, the mono- (**6**) and bimetallic fluorinated complexes (**3** and **4**) are more chemically well behaved upon oxidation. Thus, monometallic complex **6** is oxidized at a potential of 1.64 V with moderate chemical reversibility ($i_{p,c}/i_{p,a}$ = 0.65 and 0.81 at 0.1 and 1.0 V s^{-1}, respectively) while bimetallic complexes **3** and **4** display reasonably chemically reversible first oxidations ($i_{p,c}/i_{p,a}$ = 0.97 and 0.74, respectively, at 1.0 V s^{-1}) which are more electrochemically reversible ($E_{p,c} - E_{p,a}$ = 70 and 90 mV, respectively, at 1.0 V s^{-1}) than are those of **6** (see Figure 2 for the cyclic voltammogram of complex **3**). At higher scan rates (e.g. 10 V s^{-1}) both of these oxidations become fully chemically reversible ($i_{p,c}/i_{p,a} \approx 1.0$). These one-electron-oxidation processes, i.e.

$$[C_6F_4Fp_2] \underset{+e^-}{\overset{-e^-}{\rightleftharpoons}} [C_6F_4Fp_2]^{\bullet+} \qquad (9)$$

are observed at formal oxidation potentials ($E°'$) of 1.35 and 1.36 V vs SCE for **3** and **4**, respectively (at 1.0 V s^{-1}). These oxidations are clearly more chemically reversible than are those of the related perhydrophenylene derivatives **1** and **2**. The greater reversibility of the oxidations of complexes containing fluorinated alkyl and aryl groups has been noted previously and presumably reflects their greater metal–carbon bond strengths and greater steric bulk (which might slow nucleophilic attack on the radical cations). In addition, the fluorine-substituted Fp radical cations (i.e. $3^{\bullet+}$ and $4^{\bullet+}$) may also be stabilized by π donation from the lone pairs on the ortho- and para-substituted fluorine atoms, which would increase the electron density on iron and delocalize the charge to the aromatic ring. The oxidation potentials of the bimetallic complexes are observed at significantly more cathodic potentials (~ 0.3 V) than are those of the monometallic fluorobenzene complex. This shift in potentials is presumably a reflection of the substantial transfer of electron density from the Fp groups to the aromatic ring and may also be a consequence of any delocalization of charge onto the other metal center via long-range metal–metal interactions in the bimetallic complexes.

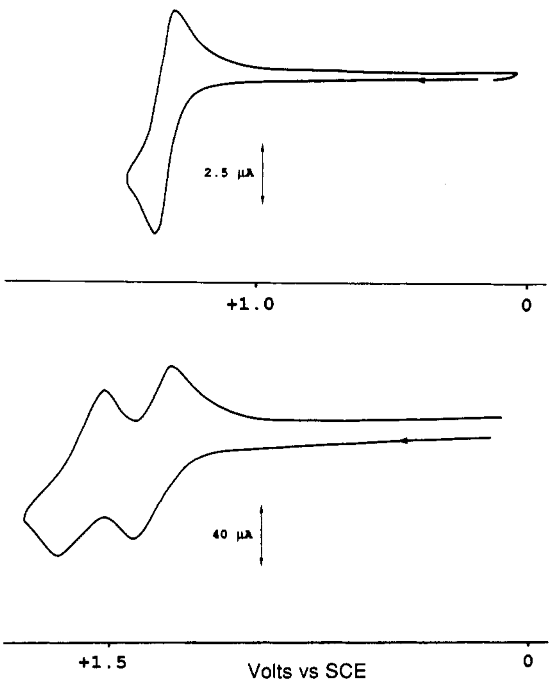

Figure 2. Cyclic voltammograms of 1,4-$C_6F_4Fp_2$ (**3**) in CH_2Cl_2 at a platinum-bead electrode: (a, top) recorded at a scan rate of 0.1 V s^{-1} and with a switching potential of 1.50 V; (b, bottom) recorded at a scan rate of 10 V s^{-1} and with a switching potential of 1.80 V.

At more anodic potentials,[29] a second one-electron-oxidation wave is observed for each bimetallic fluorophenylene complex ($E°'$ = 1.63 and 1.58 V vs SCE for **3** and **4**, respectively, at 5.0 V s^{-1}) that displays both lower chemical ($i_{p,c}/i_{p,a}$ = 0.88 and 0.71 for **3** and **4**, respectively, at 5.0 V s^{-1}) and electrochemical ($E_{p,a} - E_{p,c}$ = 120 and 150 mV for **3** and **4**, respectively, at 5.0 V s^{-1}) reversibility, i.e.

$$[C_6F_4Fp_2]^{\bullet+} \underset{+e^-}{\overset{-e^-}{\rightleftharpoons}} [C_6F_4Fp_2]^{2+} \qquad (10)$$

---

[29] All of these complexes also exhibit other oxidation waves at even higher potentials, but these lead to extensive coating of the electrode surface, making analyses of these waves difficult. These were therefore not studied in detail.

than does the first oxidation. In Figure 2, the complete cyclic voltammogram of the para-substituted complex 3 is shown as a representative example. Although the structures of these electrogenerated products are, at present, uncertain, a dimetalloquinone structure for the dication, e.g.

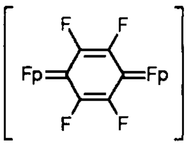

seems most reasonable since this would allow each of the iron centers to retain the favored 18-electron configuration (the individual Fe–carbene linkages being similar to those of the well-established $[Fp{=}CX_2]^+$ complexes).[30-32] Similarly, the meta-substituted dication 4^{2+} may be stabilized by quinoidal resonance interactions between each of the ortho- and para-substituted pairs of Fp and F groups. Details of the structural differences between the neutral complexes and their oxidized derivatives are likely to be very interesting, but we have, as yet, been unable to further isolate or chemically characterize these novel radical-cation or dicationic products owing to their thermal instabilities. Thus, we also cannot comment upon the degree of charge delocalization, if any, in the radical cations. Efforts are currently underway to prepare derivatives that might be expected to be more thermally stable (e.g. with C_5Me_5 and PR_3 ligands in the place of the C_5H_5 and CO ligands) so that such analyses can be carried out.

The differences observed between the first and second oxidation potentials ($\Delta E_{1/2} = |E^{\circ\prime}{}_{+1/+2} - E^{\circ\prime}{}_{0/+1}|$) of each complex are 280 and 200 mV for complexes 3 and 4, respectively (at 5.0 V s^{-1}). The magnitudes of these values can, with caution, be used as a semiquantitative measure of the magnitudes of the total metal–metal electronic interactions. They compare favorably with those observed when other first-row transition metals are bridged by the more well-studied[7,9c,14e-k] pyrazine ligand (e.g. $\Delta E_{1/2}$ for $[(CN)_5Fe]_2(\mu\text{-pyrazine})^{n-}$ = 100 mV)[14a] and indicate that the perfluorophenylene ligands (i.e. μ-C_6F_4) are able to act as relatively good electronic bridges between the metal centers. In addition, the increased magnitude of $\Delta E_{1/2}$ for the para-substituted complex compared to that for its meta analogue clearly indicates that, as expected on the basis of the ^{13}C NMR results,[11b] this electronic interaction is predominantly through-bond and not through-space. Indeed, if this interaction were occurring predominantly through-space, then the meta-substituted complex would be expected to display a larger electronic coupling than the para-substituted complex. It seems evident that the phenylene bridges in these complexes act as relatively good pathways for long-range electronic interactions between metal centers.

At intermediate scan rates, we observe more complicated than expected electrochemical behavior for complexes 3 and 4. In particular, we observe what appear to be adsorption waves (see Figure 3) arising from the second oxidations. No attempt was made to further characterize these adsorption processes.

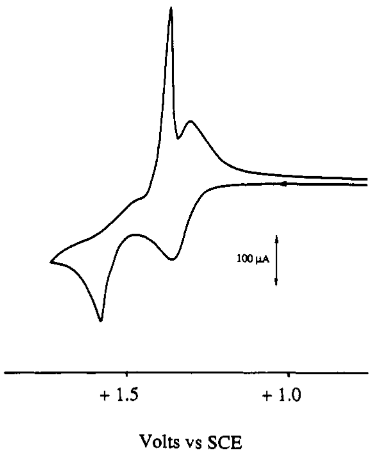

Figure 3. Cyclic voltammogram of 1,4-$C_6F_4Fp_2$ (3) in CH_2Cl_2 at a platinum-bead electrode showing the adsorption wave at a scan rate of 1.0 V s^{-1} and a switching potential of 1.78 V.

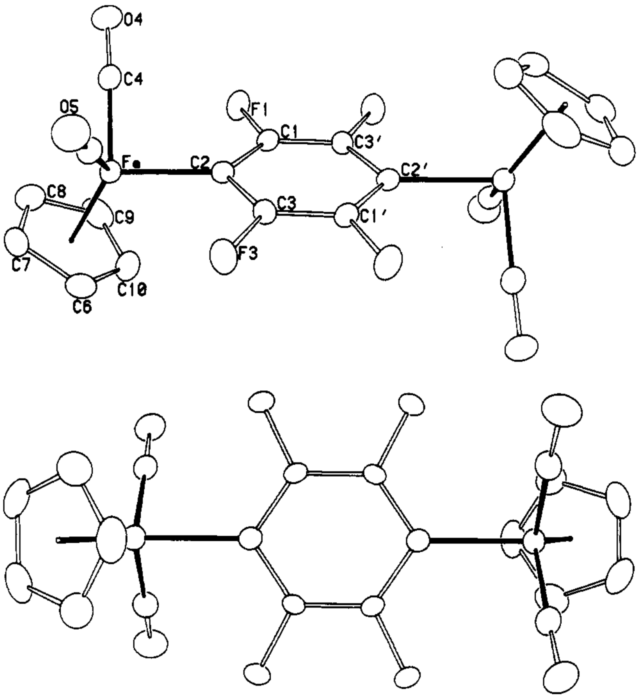

Figure 4. ORTEP plots of the complex $C_{20}H_{10}F_4Fe_2O_4$ (3): (a, top) perspective view; (b, bottom) view perpendicular to the aromatic plane.

X-ray Crystal Structure Determinations. The X-ray crystal structures of compounds $C_{20}H_{10}F_4Fe_2O_4$ (3), $C_{13}H_5F_5FeO_2$ (6), and $C_{12}H_5F_4FeNO_2$ (10) have been determined (Tables II–VI, Figures 4–6). The two monometallic complexes (i.e. Fp-C_6F_5 (6) and Fp-C_5NF_4 (10)) are isomorphous with one another, and both have crystallographically imposed mirror planes which bisect the Fp groups (Fp = $CpFe(CO)_2$) and the aromatic rings. The bimetallic complex (i.e. 1,4-$C_6F_4Fp_2$) has a crystallographically imposed inversion center which makes the halves of the molecule (i.e. Fp-C_3F_2) equivalent, and has a pseudo mirror plane, which bisects the two Fp groups and the C_6F_4 ring.

For each complex, the expected three-legged piano-stool arrangement around iron is observed and the $CpFe(CO)_2$ fragments for each of the complexes are similar (as they are by IR and NMR spectroscopy).[2,1b] Thus, each iron atom has a symmetrically bonded η^5-C_5H_5 group as well as two linear CO groups. The Fe–C(Cp) (2.075–2.105 Å), the Fe–C(carbonyl) (i.e. 1.749–1.779 Å), and the C–O distances (1.128–1.155 Å) for each complex are similar and they are unremarkable.[33-35] The Fe–C bond lengths (1.994

---

(30) Roger, C.; Lapinte, C. *J. Chem. Soc., Chem. Commun.* **1986**, 1598–1600 and references cited therein.

(31) Peng, W.-J.; Gamble, A. S.; Templeton, J. L.; Brookhart, M. *Inorg. Chem.* **1990**, *29*, 463–467 and references cited therein.

(32) O'Connor, E. J.; Helquist, P. *J. Am. Chem. Soc.* **1982**, *104*, 1869–1872 and references cited therein.

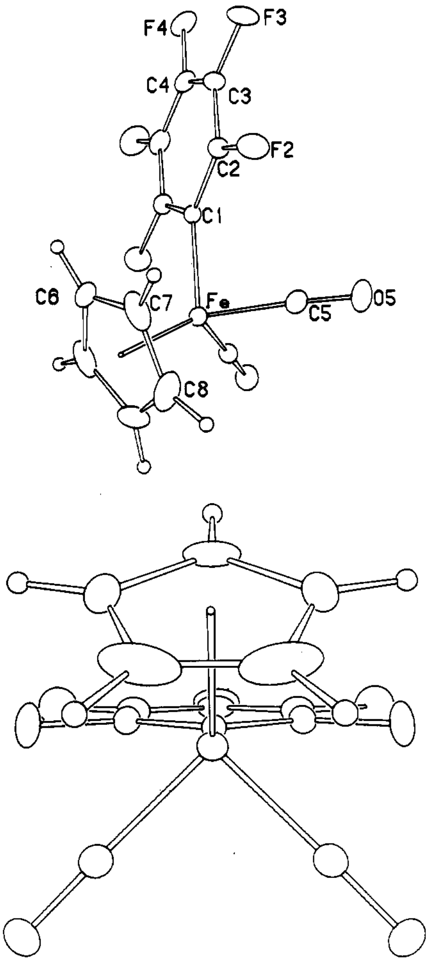

Figure 5. ORTEP plots of the complex $C_{13}H_5F_5FeO_2$ (**6**): (a, top) perspective view; (b, bottom) view along the Fe–C1 axis.

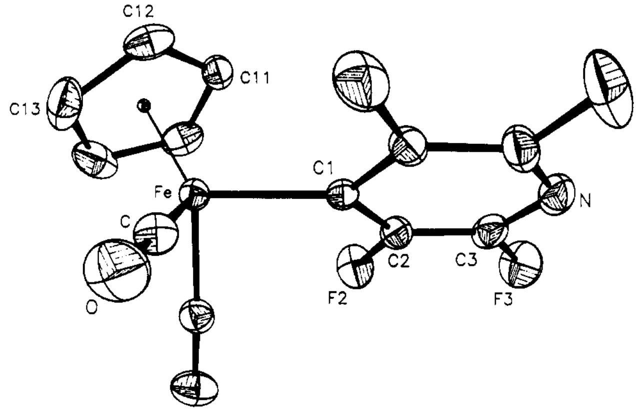

Figure 6. ORTEP plot of the complex $C_{12}H_5F_4FeNO_2$ (**10**; perspective view).

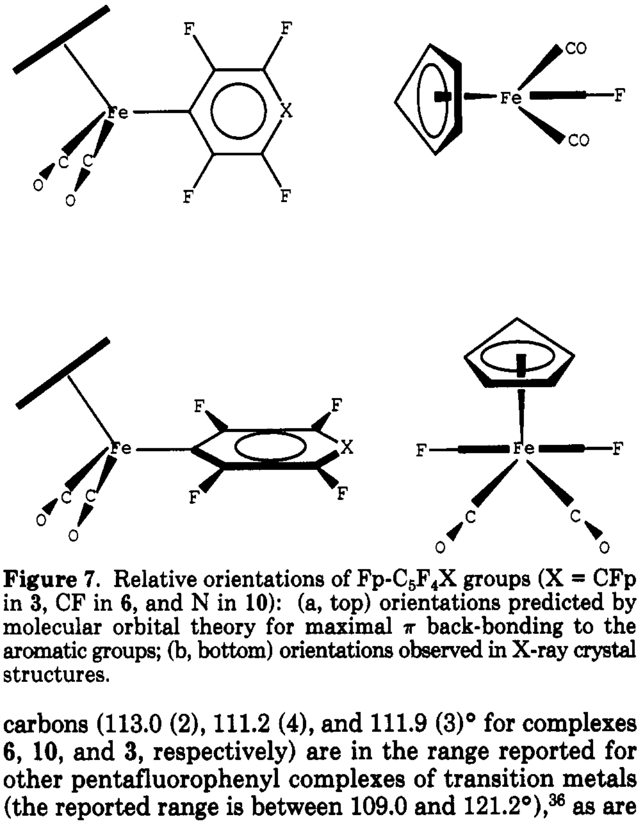

Figure 7. Relative orientations of Fp-C_5F_4X groups (X = CFp in **3**, CF in **6**, and N in **10**): (a, top) orientations predicted by molecular orbital theory for maximal π back-bonding to the aromatic groups; (b, bottom) orientations observed in X-ray crystal structures.

(4), 1.970 (4), and 2.004 (3) Å for complexes **6**, **10**, and **3**, respectively) are within the ranges reported for other complexes having both *formal* Fe–C(sp^2) single bonds (1.94–2.03 Å)[11c,33-35] and those, of cationic Fp–carbene complexes, having *formal* Fe–C(sp^2) double bonds (1.91–2.00 Å).[30] Unfortunately, the unequivocal confirmation of any Fp–arene multiple-bond character for these complexes can therefore not be made from the crystallographic data. The internal C–C–C bond angles at the ipso carbons (113.0 (2), 111.2 (4), and 111.9 (3)° for complexes **6**, **10**, and **3**, respectively) are in the range reported for other pentafluorophenyl complexes of transition metals (the reported range is between 109.0 and 121.2°),[36] as are the other aromatic bond lengths and angles.

The most interesting features of these structures are the perpendicular orientations of the aromatic rings toward the planes bisecting the Fp groups (see Figures 4–6). According to the model developed by Schilling, Hoffmann, and Lichtenberger[27] and discussed in some detail in our previous paper,[2] the $CpFe(CO)_2^+$ fragment generated from $CpFe(CO)_3^+$ contains one symmetric and one antisymmetric orbital as its two highest occupied molecular orbitals. These are both of π symmetry with respect to substituents on the $CpFe(CO)_2^+$ fragment, and both could potentially act as π-donors toward the arenes' (or azines') π^* orbitals.[2,11,27,37] The a″ HOMO of $CpFe(CO)_2^+$ is particularly well suited to such π-symmetry interactions since it is of higher energy than is the 2a′ SHOMO (second

---

[33] For structures of CpFe(CO)L aryls see: (a) Adrianov, V. G.; Sergeeva, G. N.; Streuchkov, Y. T.; Aninov, K. N.; Kolobova, N. E.; Beechastnov, A. S. *Zh. Strukt. Khim.* **1970**, *11*, 168–169; *J. Struct. Chem.* (*Engl. Transl.*) **1970**, *11*, 163–164. (b) Lehmkuhl, H.; Mehler, G.; Benn, R.; Rufinska, A.; Schroth, G.; Kruger, C.; Raabe, E. *Chem. Ber.* **1987**, *120*, 1987. (c) Semion, V. A.; Struchkov, Y. T. *Zh. Strukt. Khim.* **1969**, *10*, 88–94 *J. Struct. Chem.* (*Engl. Transl.*) **1969**, *10*, 80–85.

[34] For structures of Fp–R (where R is sp^2 hybridized) see: (a) Churchill, M. R.; Wormald, J. *Inorg. Chem.* **1969**, *8*, 1936–1941. (b) Ferede, R.; Noble, M.; Cordes, A. W.; Allison, N. T.; Lay, J., Jr. *J. Organomet. Chem.* **1988**, *399*, 1–6. (c) Bruce, M. I.; Liddell, J. J.; Snow, M. R.; Teikink, E. R. T. *J. Organomet. Chem* **1988**, *354*, 103–115. (d) Dahl, L. F.; Doedena, R. J.; Huble, W.; Nielson, J. *J. Am. Chem. Soc.* **1966**, *88*, 446–452. (e) Kolobova, N. E.; Rozaantava, T. V.; Struchkov, Y. T.; Betaanov, A. S.; Bakmutov, V. I. *J. Organomet. Chem.* **1985**, *292*, 247–256.

[35] For structures of Fp–Ar (where the aryl is π bound to 12-electron metal center) and related species, see: (a) Reference 11a. (b) Heppert, J. A.; Morgenstern, M. A.; Scherubel, D. M.; Takusagawa, F.; Shaker, M. R. *Organometallics* **1988**, *7*, 1715–1723. (c) Heppert, J. A.; Thomas-Miller, M. E.; Swepston, P. N.; Extin, M. W. *J. Chem. Soc., Chem. Commun.* **1988**, 280–282. (d) Casey, C. P.; Konings, M. S.; Gohdes, M. A.; Meszaros, M. W. *Organometallics* **1988**, *7*, 2103–2107. (e) Batsanov, A. S.; Struchkov, Yu. T. *J. Organomet. Chem.* **1984**, *266*, 295–301. (f) Nametkin, N. S.; Tyurin, V. D.; Nekhaev, A. I.; Sobolev, Y. P.; Kondrat'eva, M. G.; Batsanov, A. S.; Struchkov, Yu. T. *J. Organomet. Chem.* **1983**, *243*, 323–330.

[36] Jones, P. G. *J. Organomet. Chem.* **1988**, *345*, 405–411.

[37] For calculations on related systems, see: (a) Reference 27. (b) Schilling, B. E. R.; Hoffmann, R.; Faller, J. W. *J. Am. Chem. Soc.* **1979**, *101*, 592–598. (c) Seeman, J. I.; Davies, S. G. *J. Am. Chem. Soc.* **1985**, *107*, 6522–6531. (d) Crocco, G. L.; Gladysz, J. A. *J. Am. Chem. Soc.* **1988**, *110*, 6110–6118 and work cited therein.

Organometallics 1992, *11,* 597–601

highest occupied molecular orbital). Fp–arene (and by logical extension Fp–azine) complexes are expected[27] to adopt geometries having Fp–substituent orientations which maximize overlap between the a″ HOMO and the aromatic π^*-acceptor orbitals. Indeed, this electronic preference would be expected to be stronger for the more strongly π-accepting[2,11] fluorinated aromatics than it is for the C_6H_5 group used in the calculations. In the case of σ-bonded aromatic ligands, these calculations predict a geometry in which the aromatic ring is coplanar with the mirror plane or pseudo mirror plane of the Fp fragment(s) (i.e. Figure 7a). Surprisingly, in these complexes (Figures 4–6) the aromatic rings are observed to have the opposite orientations in which the aromatic planes are perpendicular to the Fp mirror planes or pseudo mirror planes (i.e. Figure 7b). We do not believe that crystal-packing effects can account for this orientational preference, since no unusual intermolecular contacts are observed. In addition, this orientational preference is observed for a wide variety of different complexes and crystal environments.[38] This observation suggests that, at least in the solid state, the major π interaction involves the Fp^+ 2a′ orbitals donating to the aromatic LUMO's, since this is the only type of π-symmetry overlap available for the observed perpendicular orientations. Since the 2a′ orbital is of lower energy than a″ and is therefore presumably a poorer π donor, the explanation for the observed orientational preference shown in Figure 7b is unlikely to be electronic in nature.[39] Indeed, qualitative molecular modeling studies[40] indicate that adverse steric interactions between the ortho substituents on the aromatic rings and the other ligands on the iron atoms are much smaller at the crystallographically observed orientations than they are at the orientations predicted by molecular orbital theory.[41]

Acknowledgment. We gratefully acknowledge the Natural Sciences and Engineering Research Council of Canada and the University of Alberta (R.C., A.D.H., and B.D.S.) and the National Science Foundation (S.G.B., J.L.A., and J.C.) for their financial support of this work. We also thank Dr. George B. Richter-Addo for his contributions to the electrochemical studies.

Registry No. **1**, 119945-86-7; **2**, 119970-49-9; **3**, 37366-22-6; $\mathbf{3}^+$, 137007-60-4; $\mathbf{3}^{2+}$, 137007-67-1; **4**, 37355-34-3; $\mathbf{4}^+$, 137007-61-5; $\mathbf{4}^{2+}$, 137007-66-0; **5**, 12126-73-7; **6**, 12176-60-2; $\mathbf{6}^+$, 137007-62-6; **7**, 31781-18-7; **8**, 33136-08-2; **9**, 33072-10-5; $\mathbf{9}^+$, 137007-63-7; **10**, 12129-49-6; $\mathbf{10}^+$, 137007-64-8; **11**, 134705-81-0; $\mathbf{11}^+$, 137038-76-7; **12**, 134705-82-1; $\mathbf{12}^+$, 137007-65-9; **13**, 134705-80-9; **14**, 134705-73-0; **15**, 134705-68-3; **16**, 134705-74-1; **17**, 134705-76-3; **18**, 134705-78-5; NaFp, 12152-20-4; 1,2,3,5-$C_6H_2F_4$, 2367-82-0; 1,4-C_6H_4FBr, 460-00-4; FpI, 12078-28-3; *n*-BuLi, 109-72-8; [*n*-Bu_4N]PF_6, 3109-63-5; Pt, 7440-06-4; CH_2Cl_2, 75-09-2; 1,3-$C_6H_2F_4$, 2367-82-0.

Supplementary Material Available: Complete descriptions of the X-ray crystal structure determinations and tables of atomic coordinates and anisotropic Gaussian parameters, bond lengths, bond angles, hydrogen atom coordinates and Gaussian parameters, least-squares planes, torsional angles, and root-mean-square amplitudes of vibration for 3, 6, and 10 (22 pages); listings of structure factor amplitudes (27 pages). Ordering information is given on any current masthead page.

---

(38) Similar orientations are observed in numerous related arene and azine derivatives.[2,11c,35]

(39) The predictions of these and similar calculations have proven to be very reliable predictors of other metal–arene orientations in the past;[27,37] however, no similar *intra*molecular steric interactions are expected for these other systems.

(40) Using the program Chem 3D$^+$ from Cambridge Scientific Computing and the crystallographically derived internal coordinates for the molecules.

(41) The electronically preferred orientations result in unreasonably short intramolecular H(Cp)–F(aromatic) nonbonded contacts of ~2.0 Å.

Silicon–Carbon Unsaturated Compounds. 37. Thermal Behavior of 1-Mesityl-3-phenyl-1,2-bis(trimethylsilyl)silacyclopropene

Mitsuo Ishikawa,*,[1a] Tomoyuki Horio,[1a] Yukiharu Yuzuriha,[1a] Atsutaka Kunai,[1a]
Tomitake Tsukihara,*,[1b] and Hisashi Naitou[1c]

Department of Applied Chemistry, Faculty of Engineering, Hiroshima University, Higashi-Hiroshima 724, Japan, Department of Biological Science and Technology, Faculty of Engineering, Tokushima University, Minamijyosanjima, Tokushima 770, Japan, and Department of Applied Chemistry, Osaka University, Yamada-Kami, Suita 565, Japan

Received June 12, 1991

The thermolysis of 1-mesityl-3-phenyl-1,2-bis(trimethylsilyl)silacycloprop-2-ene (1) at 250 °C afforded 1-mesityl-3,3-dimethyl-4-phenyl-5-(trimethylsilyl)-1,3-disilacyclopent-4-ene (2) and 1-mesityl-1,3-bis(trimethylsilyl)-1-silaindene (3). Similar thermolysis of 1 in the presence of phenyl(trimethylsilyl)acetylene produced *cis*- and *trans*-7a-mesityl-1-phenyl-2,2a,7-tris(trimethylsilyl)cyclobutenosilaindan (7 and 8), together with 2 and 3. When compound 1 was heated with methyldiphenylsilane under the same conditions, 2-mesityl-1,3,3,3-tetramethyl-1,1-diphenyltrisilane and (*E*)-1-(1-mesityl-2-methyl-2,2-diphenyldisilanyl)-1,2-bis(trimethylsilyl)-2-phenylethene were obtained, in addition to the products 2 and 3. *cis*-Cyclobutenosilaindan 7, $C_{34}H_{48}Si_4$ crystallizes in the space group $P\bar{1}$ with cell dimensions a = 11.186 (1) Å, b = 17.105 (1) Å, c = 10.208 (1) Å, α = 107.37 (1)°, β = 87.92 (1)°, γ = 109.63 (1)°, V = 1751.3 (3) Å^3, and D_{calcd} = 1.02 g/cm^3 (Z = 2).

Introduction

The silapropadienes which are useful intermediates for the preparation of silicon-containing small-ring compounds can be readily synthesized by the photolysis of phenylethynylpolysilanes.[2-5] Recently, we have found that the reaction of phenylethynylpolysilanes and their photoi-

---

(1) (a) Hiroshima University. (b) Tokushima University. (c) Osaka University.

(2) Ishikawa, M.; Kovar, D.; Fuchikami, T.; Nishimura, K.; Kumada, M.; Higuchi, T.; Miyamoto, S. *J. Am. Chem. Soc.* **1981**, *103*, 2324.

(3) Ishikawa, M.; Nishimura, K.; Ochiai, H.; Kumada, M. *J. Organomet. Chem.* **1982**, *236*, 7.

0276-7333/92/2311-0597$03.00/0